



Original article

Regulation of drug release performance using mixed doxorubicin-doxorubicin dimer nanoparticles as a pH-triggered drug self-delivery system



Jiagen Li, Xinming Li, Pengwei Xie, Peng Liu*

State Key Laboratory of Applied Organic Chemistry, College of Chemistry and Chemical Engineering, Lanzhou University, Lanzhou, 730000, China

ARTICLE INFO

Article history:

Received 3 August 2020

Received in revised form

25 February 2021

Accepted 5 March 2021

Available online 9 March 2021

Keywords:

Drug self-delivery system

Regulated drug release

Doxorubicin-doxorubicin dimer

Acid-triggered release

Mixed nanoparticles

ABSTRACT

A mixed drug self-delivery system (DSDS) with high drug content (>50%) was developed to regulate pH-triggered drug release, based on two doxorubicin (DOX)-DOX dimers: D-DOX_{ADH} and D-DOX_{car} conjugated with acid-labile dynamic covalent bonds (hydrazone and carbamate, respectively) and stabilized with PEGylated D-DOX_{ADH} (D-DOX_{ADH}-PEG). Owing to the different stability of the dynamic covalent bonds in the two dimers and the noncovalent interaction between them, pH-triggered drug release could be easily regulated by adjusting the feeding ratios of the two DOX-DOX dimers in the mixed DSDS. Similar in vitro cellular toxicity was achieved with the mixed DSDS nanoparticles prepared with different feeding ratios. The mixed DSDS nanoparticles had a similar DOX content and diameter but different drug releasing rates. The MTT assays revealed that a high anti-tumor efficacy could be achieved with the slow-release mixed DSDS nanoparticles.

© 2021 Xi'an Jiaotong University. Production and hosting by Elsevier B.V. This is an open access article under the CC BY-NC-ND license (<http://creativecommons.org/licenses/by-nc-nd/4.0/>).

1. Introduction

Doxorubicin (DOX), a broad-spectrum chemotherapeutic agent, has been widely used for cancer treatment [1]. However, it usually presents severe toxic side effects on normal cells and tissues because of its non-specificity [2]. Therefore, tumor specific drug delivery systems (DDSs) have been investigated intensely for DOX to improve its anti-tumor efficacy and minimize its toxic side effects on normal cells and tissues, in the form of DOX-loaded nanocarriers via non-covalent interactions (such as electrostatic or hydrophobic interaction, π - π stacking, or hydrogen bonds) [3], or as prodrugs via acid-labile or reduction-cleavable dynamic covalent bonds [4].

Owing to the acid-labile or reduction-cleavable dynamic covalent conjugations in the prodrugs, which can be cleaved to release the drug upon stimuli of acid or a high reductant level in the tumor cells, minimized premature drug leakage can be achieved to avoid the toxic side effects. Therefore, these prodrugs have attracted increasing attention in the last decades [4]. For the DDSs, the particle shape and size and surface property mainly affect their

internalization into the tumor cells [5], whereas the drug content and drug releasing rate are the main factors determining anti-tumor efficacy. Particularly, after cellular uptake, a low intracellular drug concentration is usually achieved with the DDSs with low drug content. Moreover, the low intracellular drug concentration can barely kill the tumor cells but might cause multidrug resistance [6].

Compared with the high anti-tumor efficacy of DOX released from the acid-labile prodrugs, the low anti-tumor efficacy has been achieved for the reduction-cleavable prodrugs, because the released drug is usually a thiolated derivative of DOX [7]. Furthermore, in most of the reported tumor-specific polymer prodrugs, the chemotherapeutic agents such as DOX are usually conjugated onto the side groups or end groups of the polymer chains [8]; thus, it is a pity that only a low drug content could be obtained. Therefore, the development of an acid-labile prodrug with high drug content but low premature drug leakage is urgent for cancer treatment.

Most recently, drug self-delivery systems (DSDSs), also known as cargo-free nanomedicines, have drawn much attention for cancer treatment, achieving intracellular delivery on their own without any nanocarriers [9]. With the desired high drug content similar to that in the drug nanocrystals [10], the dimer prodrugs exhibit a lower premature drug leakage than the pure chemotherapeutics owing to their lower solubility. However, the drug

Peer review under responsibility of Xi'an Jiaotong University.

* Corresponding author.

E-mail address: pliu@lzu.edu.cn (P. Liu).

releasing rate is mainly determined by the acid-labile dynamic covalent bond in the dimers, in addition to the diameters of the DSDSs [11,12].

Besides the high drug content, the drug releasing rate is another key factor in controlling the anti-tumor efficacy of the DDSs [13]. Till date, different strategies have been established to modulate the drug releasing rate such as dual-modal drug-loading [14,15] or tuning the surface textures of the drug-carriers [16]. As an ideal acid-labile DSDS with high drug content, the chemotherapeutic drug is expected to be released at a desired rate to kill the cancer cells.

In the present study, novel DSDS nanoparticles with high drug content (>50%) were developed to regulate the pH-triggered drug release, by stabilizing two DOX-DOX dimers conjugated with acid-labile dynamic covalent bonds: D-DOX_{ADH} via a hydrazone bond with a rapid DOX releasing rate and D-DOX_{car} via a carbamate bond with a slow DOX releasing rate, with the PEGylated D-DOX_{ADH} (D-DOX_{ADH}-PEG) as an emulsifier (Scheme 1). Different DOX releasing rates, despite similar DOX content and diameter, were achieved by adjusting the feeding ratios of the two DOX-DOX dimers in the proposed DSDS. In addition, all the proposed DSDSs exhibited the enhanced anti-tumor efficacy on HepG2 cells in comparison to that with the free DOX.

2. Experimental

2.1. Reagents and chemicals

mPEG-COOH (95%, weight-average molecular weight = 2000 Da) was purchased from Shanghai Biotech Co., Ltd. (Shanghai, China). Doxorubicin hydrochloride (DOX·HCl, 99.4%) was purchased from Beijing Huafang United Technology Co., Ltd. (Beijing, China). 1,5-Pentanediol (98%) was obtained from Chengdu Chron Chemicals Co., Ltd. (Chengdu, China). 4-Nitrophenyl chloroformate (98%) was obtained from J&K Chemical Ltd. (Beijing, China). Adipic acid dihydrazide (ADH, 98%), *N*-(3-dimethylaminopropyl)-*N'*-

Table 1

Doxorubicin (DOX) content of the mixed drug self-delivery system (DSDS) nanoparticles (D-DOX_{mix} NPs) prepared with different feeding ratios.

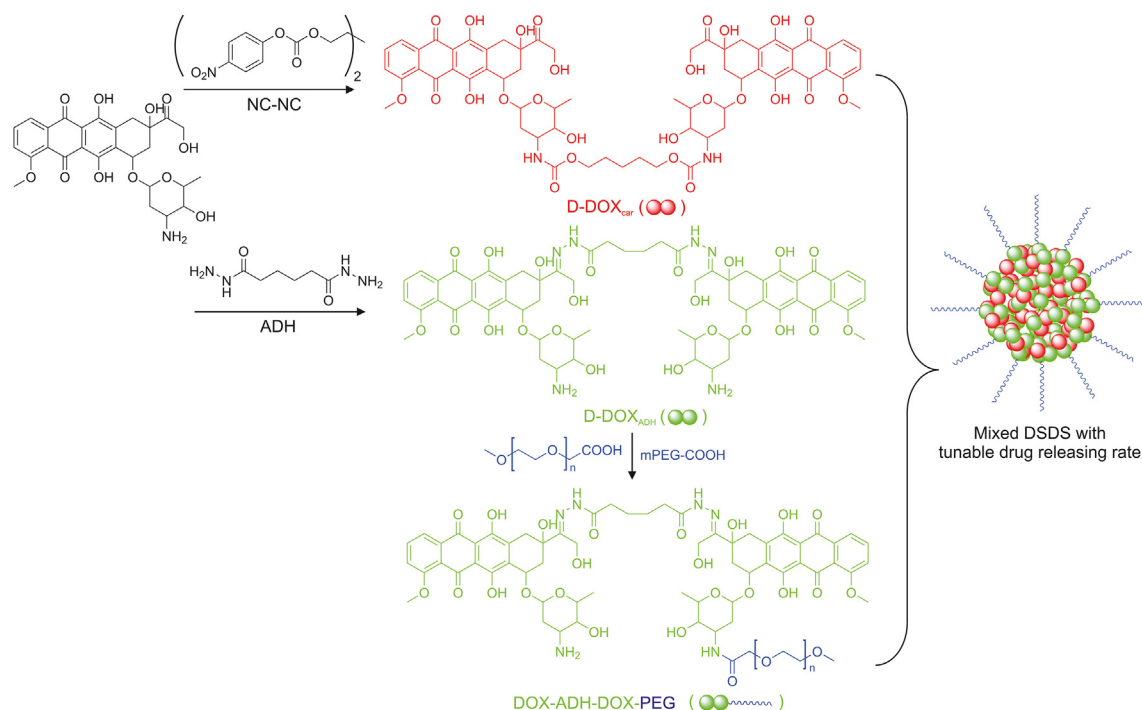
DSDSs	Feeding ratios (D-DOX _{car} :D-DOX _{ADH} :D-DOX _{ADH} -PEG, mg/mg/mg)	DOX content (%)
D-DOX _{mix} -1	0:10:10	56.73
D-DOX _{mix} -2	2.5:7.5:10	58.51
D-DOX _{mix} -3	5:5:10	59.50
D-DOX _{mix} -4	7.5:2.5:10	57.86
D-DOX _{mix} -5	10:0:10	60.33
D-DOX _{mix} -3a	5:0:10	51.07
D-DOX _{mix} -3b	0:5:10	52.61

ethylcarbodiimide hydrochloride (99%), 1-hydroxybenzotriazole (99%), and 4-dimethylaminopyridine (99%) were purchased from J&K Chemical Ltd. (Beijing, China). All other reagents and solvents were of analytical grade and used without further purification. Double distilled water was used throughout the experiments.

2.2. Preparation and characterization of mixed DSDS nanoparticles

D-DOX_{car} via an acid-labile carbamate linker with a DOX content of 86.59% was synthesized by conjugating two DOX molecules with one bis(4-nitrophenyl) pentane-1,5-diyl bis(carbonate) molecule as reported previously [11]. ¹H NMR (400 MHz, dimethyl sulfoxide DMSO-*d*₆, Fig. S1): δ 1.54–1.40 (f, 6.00H), 4.03–3.76 (a + e, 10.02H), 7.66–7.53 (c, 2.01H), 7.96–7.81 (b + d, 4.00H).

D-DOX_{ADH} via an acid-labile hydrazone linker with a DOX content of 88.76% was synthesized by conjugating DOX molecules with ADH as described previously [12]. ¹H NMR (400 MHz, DMSO-*d*₆, Fig. S2): δ 4.02–3.89 (a, 6.00H), 2.22–2.08 (b, 4.01H), 1.62–1.48 (c, 3.96H). The D-DOX_{ADH}-PEG with a DOX content of 33.92% was synthesized as an emulsifier by the PEGylation of D-DOX_{ADH} with



Scheme 1. Preparation of the mixed drug self-delivery system (DSDS) nanoparticles. ADH: adipic acid dihydrazide; DOX: doxorubicin.

mPEG-COOH [12]. ^1H NMR (400 MHz, DMSO- d_6 , Fig. S3): δ 3.63–3.44 (b, 176.00H), 4.05–3.90 (a, 5.95H).

Then, the mixed DSDS nanoparticles (D-DOX_{mix} NPs) were prepared by emulsifying the two DOX-DOX dimers, D-DOX_{car} and D-DOX_{ADH}, at different feeding ratios, with D-DOX_{ADH}-PEG as the emulsifier (Table 1). Taking D-DOX_{mix}-3 as an example, D-DOX_{car} (5.00 mg), D-DOX_{ADH} (5.00 mg), and D-DOX_{ADH}-PEG (10.00 mg) were dissolved in 5.00 mL of DMSO. Then the solution was added drop-by-drop to 50 mL water with violent stirring. After stirring for 5 min, the D-DOX_{mix}-3 NPs were collected by centrifugation (10,000 r/min for 5 min), washed with water, and dried in vacuum at 40 °C.

Through sampling with their aqueous dispersions, the particle morphology and hydrodynamic diameter of the obtained D-DOX_{mix} NPs were characterized using transmission electron microscope (TEM, Talos F200c, Thermo Fisher Scientific, Waltham, MA, USA) and dynamical light scattering (DLS, BI-200SM, Brookhaven Instruments Corp., Holtsville, NY, USA), respectively.

The DOX content of the obtained DOX-DOX dimer and D-DOX_{mix} NPs was determined in a 0.02 mg/mL DMSO solution with a UV–vis spectrometer (Lambda 35, PerkinElmer, Inc. Shelton, CT, USA) with absorbance at 480 nm, and calculations based on the standard curve of DOX·HCl in DMSO [11,12].

2.3. Acid-triggered drug release

Ten milliliters of the dispersion of the D-DOX_{mix} NPs (0.20 mg/mL) in different buffer solutions (phosphate-buffered saline (PBS) at pH 7.4 or acetate-buffered solution (ABS) at pH 5.0) was transferred into a dialysis bag (molecular weight cut-off of 1 kD). The dialysis bag was then immersed in the corresponding buffer solution (100 mL). After a predetermined time, 5.0 mL of the dialysate was removed to measure the concentration of the released DOX using the UV–vis spectrometer (Lambda 35, PerkinElmer, Inc. Shelton, CT, USA) at an absorbance wavelength of 480 nm. Fresh solution (5.0 mL) was added to keep the total volume constant.

2.4. In vitro cellular toxicity and uptake

HepG2 cells were used as model tumor cells after cultivation on 96-well plates (1.0×10^5 cells/well) in 100 μL of Dulbecco's modified Eagle's medium containing 10% fetal bovine serum and incubation in atmospheric humidity (5% CO₂, 95% air, 37 °C) for 24 h.

The in vitro cytotoxicity of the proposed D-DOX_{mix} NPs was evaluated via the MTT assay. After the HepG2 cells were incubated with the D-DOX_{mix} NPs or free DOX at different concentrations for 24 h, 20.0 μL of 5.0 mg/mL MTT was added into each well, for further incubation of 4 h. Then, the MTT-containing medium was removed and replaced with 150 μL of DMSO. After the crystal substances were dissolved for 20 min in each well, the absorbance of the solution was measured at 490 nm on a microplate reader.

The in vitro cellular uptake of the D-DOX_{mix}-3 NPs was examined using confocal laser scanning microscopy (DMI 4000B, Leica, Wetzlar, Germany) after incubating the HepG2 cells with 15 $\mu\text{g}/\text{mL}$ D-DOX_{mix}-3 NPs for 24 h. The cells were washed with the culture solution, fixed with 4% paraformaldehyde, and dyed with 4',6-diamidino-2-phenylindole (DAPI). The fluorescence was analyzed at 480 nm for DOX and 461 nm for DAPI.

2.5. Statistical analysis

All data are presented as mean \pm standard deviation. The statistical analyses were performed with the one-way ANOVA and the Student's *t*-test was used for two-group comparisons (SPSS software, version 16.0, SPSS Inc.; Chicago, IL, USA). Statistical significance was set at $P < 0.05$.

3. Results and discussion

3.1. Preparation and characterization of mixed DSDS nanoparticles

Because of the hydrophobicity of the two dimers, as well as the anthracene rings, they could precipitate in water via noncovalent interactions, such as the hydrophobic interaction and π - π stacking interaction. The D-DOX_{mix} NPs were prepared as mixed DSDS NPs by stabilizing the slow-releasing D-DOX_{car} and the fast-releasing D-DOX_{ADH} at different feeding ratios with D-DOX_{ADH}-PEG as the emulsifier (Scheme 1).

The mean hydrodynamic diameters (D_h) of the D-DOX_{mix} NPs were less than 200 nm (Fig. 1), indicating that the D-DOX_{mix} NPs could be passively targeted to tumor sites via the enhanced permeability and retention effect. With an increase in the feeding ratio of D-DOX_{car} with D-DOX_{car}:D-DOX_{ADH}:D-DOX_{ADH}-PEG from 0:10:10 to 2.5:7.5:10, 5:5:10, 7.5:2.5:10, and 10:0:10 (mg/mg/mg), it was clear that the D_h decreased from 194 nm for the D-DOX_{mix}-1 NPs to 187 nm for the D-DOX_{mix}-2 NPs, 180 nm for the D-DOX_{mix}-3 NPs, 161 nm for the D-DOX_{mix}-4 NPs, and finally, 125 nm for the D-DOX_{mix}-5 NPs (Fig. 1). This might be owing to the different hydrophilic-hydrophobic properties of the two DOX-DOX dimers. D-DOX_{ADH} was synthesized by conjugating DOX on its carbonyl group with ADH and the amino group in DOX was retained; therefore, it should have a higher hydrophilic property than the D-DOX_{car} conjugated on the amino group in DOX.

In the TEM analysis, all the mixed DSDS NPs showed a near spherical shape. Similar to the results with the DLS, the particle size decreased from 90 nm for the D-DOX_{mix}-1 NPs (Fig. 2A) to 78 nm for the D-DOX_{mix}-2 NPs (Fig. 2B), 65 nm for the D-DOX_{mix}-3 NPs (Fig. 2C), 60 nm for the D-DOX_{mix}-4 NPs (Fig. 2D), and finally, 43 nm for the D-DOX_{mix}-5 NPs (Fig. 2E), with the increase in the feeding ratio of D-DOX_{car}. The D_h from the DLS analysis was much higher than that of the particle size from TEM analysis owing to surface PEG brushes in the D-DOX_{ADH}-PEG, as well as the solvation of the DOX-DOX dimers.

The DOX content of the D-DOX_{mix} NPs prepared with different feeding ratios was determined using a UV–vis spectrometer and is listed in Table 1. With the different D-DOX_{car}:D-DOX_{ADH}:D-DOX_{ADH}-PEG feeding ratios, the DOX content of the D-DOX_{mix} NPs was in the range of 56%–60%. In addition, the determined DOX content was close to the theoretical values calculated from the corresponding DOX content of the components at certain feeding ratios, demonstrating a high yield in the emulsification.

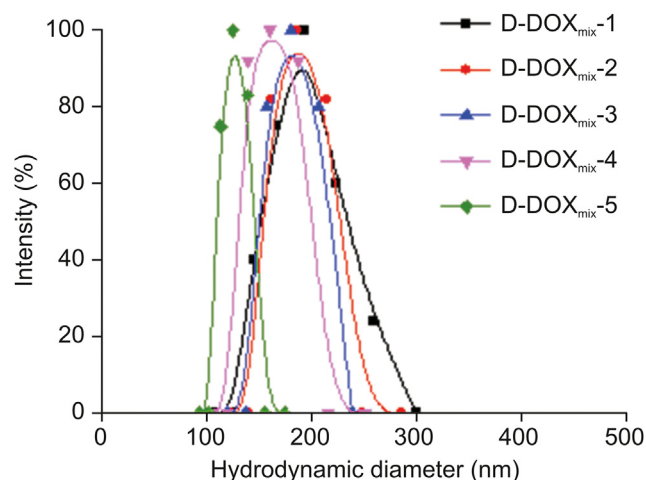


Fig. 1. Typical hydrodynamic diameter distributions of the mixed drug self-delivery system nanoparticles (D-DOX_{mix} NPs) in pH 7.4 phosphate-buffered saline.

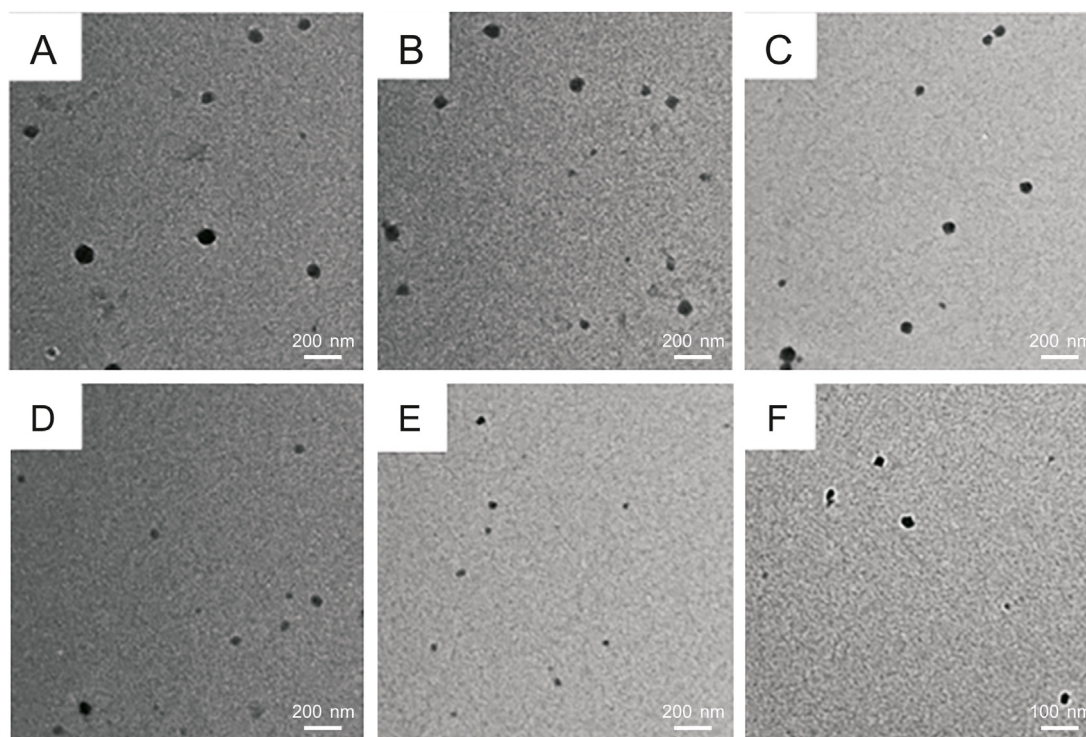


Fig. 2. Transmission electron microscopy images of (A) the D-DOX_{mix}-1 NPs, (B) D-DOX_{mix}-2 NPs, (C) D-DOX_{mix}-3 NPs, (D) D-DOX_{mix}-4 NPs, (E) D-DOX_{mix}-5 NPs in pH 7.4 phosphate-buffered saline, and (F) the D-DOX_{mix}-3 NPs after treating with pH 5.0 acetate-buffered solution for 36 h.

3.2. pH-triggered drug release profiles

The acid-triggered drug release profiles of the D-DOX_{mix} NPs were evaluated in the different releasing media, pH 7.4 PBS and pH 5.0 ABS, mimicking the normal physiological media and tumor intracellular microenvironment, respectively. The effect of the emulsifier D-DOX_{ADH}-PEG on the drug release behavior was first investigated by comparing the drug release profiles of the pure D-DOX_{car} NPs and D-DOX_{ADH} NPs with the emulsified ones (D-DOX_{mix}-3a NPs and D-DOX_{mix}-3b NPs). As shown in Fig. 3A, the D-DOX_{mix}-3b NPs showed a much lower drug leakage of 6.85% than the 13.30% of pure D-DOX_{ADH} NPs in pH 7.4 PBS. This was because the D-DOX_{ADH}-PEG in the D-DOX_{mix}-3b NPs could be slightly cleaved to release DOX and DOX-PEG; the former could diffuse through the dialysis bag and be determined in the dialysate, whereas the latter remained in the dialysis bag owing to its higher molecular weight.

Regarding the D-DOX_{car} dimer, the D-DOX_{mix}-3a NPs showed a slightly higher drug leakage of 2.41% than the 2.11% of pure D-DOX_{car} NPs. The carbamate bond in the D-DOX_{car} dimer is a dynamic covalent bond with higher stability than that of the hydrazone bond in the D-DOX_{ADH} dimer [17]. Therefore, it was used for the intracellular pH-triggered slow DOX release to eradicate any residual or latent cancer cells that lead to the recurrence of tumor [11]. However, the D-DOX_{ADH}-PEG in the D-DOX_{mix}-3a NPs could be cleaved to release DOX.

In the pH 5.0 ABS mimicking the tumor intracellular microenvironment, the D-DOX_{mix}-3b NPs gave a lower drug release of 66.75% than the pure D-DOX_{ADH} NPs, whereas the D-DOX_{mix}-3a NPs showed a slightly higher drug release of 5.40% than the pure D-DOX_{car} NPs, similar to the drug release profiles in the pH 7.4 PBS mimicking the normal physiological media. This demonstrated that the drug release performance was mainly determined by the DOX-DOX dimers. To be precise, it was dependent on the dynamic covalent conjugating bonds in the DOX-DOX dimers.

Next, the effect of the feeding ratios of D-DOX_{car} and D-DOX_{ADH} on the acid-triggered drug release from the D-DOX_{mix} NPs was investigated. The results are shown in Fig. 3B. With increasing feeding ratio of the slow-release dimer D-DOX_{car}, the drug leakage at pH 7.4 and drug release at pH 5.0 decreased noticeably. The results demonstrated that the drug release rate could be efficiently modulated by adjusting the feeding ratio of the slow-releasing dimer D-DOX_{car}. Comparison of the drug release profiles of the D-DOX_{mix}-3b and D-DOX_{mix}-3 NPs, both possessing the same D-DOX_{ADH}:D-DOX_{ADH}-PEG feeding ratio of 5:10 (mg/mg), showed that the D-DOX_{mix}-3 NPs with a higher drug content (59.50%) had a lower drug release amount (drug content × cumulative drug release) of 0.25 mg/mg in pH 5.0 ABS within 36 h, whereas the D-DOX_{mix}-3b NPs with a lower drug content (52.61%) showed a higher drug release amount of 0.35 mg/mg. These results indicate that the regulated drug release rate was ascribed to not only the slow drug release rate from the slow-releasing dimer D-DOX_{car}, but also the inter-molecular noncovalent interaction between the DOX-DOX dimers. Owing to the noncovalent interaction, the cleavage of the fast-releasing dimer D-DOX_{ADH} was reduced by the slow-releasing dimer D-DOX_{car}. These two factors, both the slow release rate from D-DOX_{car} and the restricted release rate from D-DOX_{ADH} owing to the noncovalent interaction with the D-DOX_{car}, determined the drug release rate from the proposed mixed DSDSs.

Taking the D-DOX_{mix}-3 NPs as an example, which were prepared with a D-DOX_{car}:D-DOX_{ADH}:D-DOX_{ADH}-PEG feeding ratio of 5:5:10 (mg/mg/mg), they remained in a spherical shape with a small size after treatment with pH 5.0 ABS for 36 h, without breaking into small pieces that could be produced during the potential disintegration of the D-DOX_{mix}-3 NPs (Fig. 2F). Based on this phenomenon, the drug releasing mechanism could be speculated as follows: first, the H⁺ cations attacked the hydrazone bond on the surface D-DOX_{ADH}-PEG layer to produce DOX and DOX-PEG and DOX was released into the releasing medium. Then, the H⁺ cations diffused slowly into the hydrophobic cores of the D-DOX_{mix}-3 NPs and

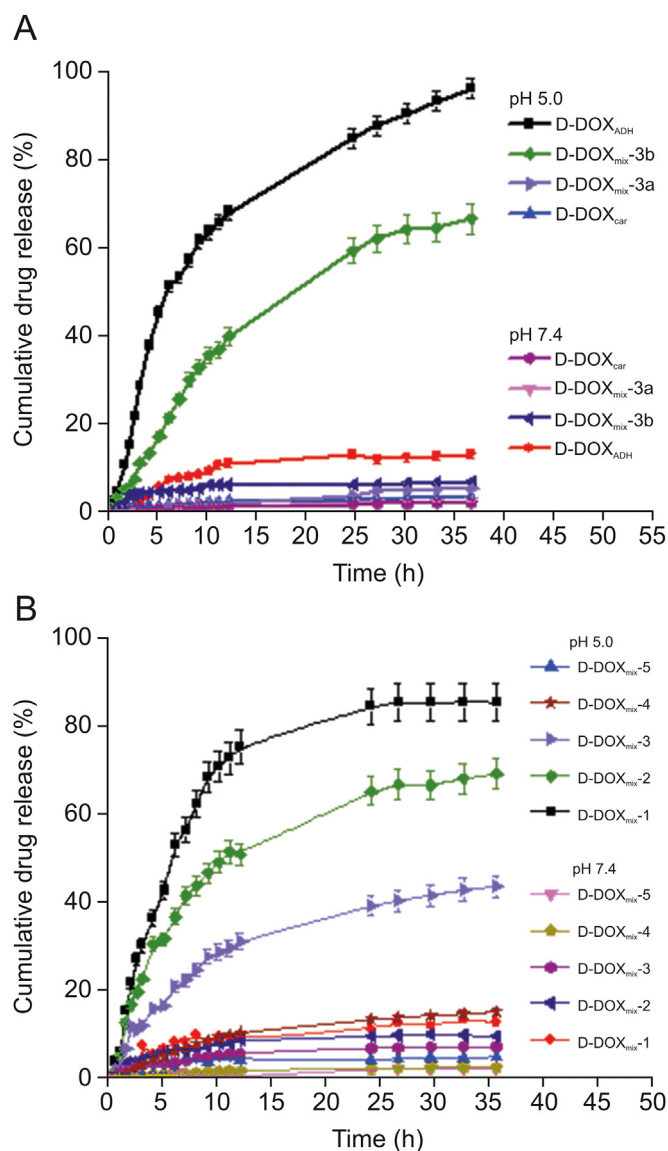


Fig. 3. Acid-triggered drug release profiles of the D-DOX_{mix} NPs: effects of (A) the emulsifier D-DOX_{ADH}-PEG and (B) the feeding ratios of the D-DOX_{car} and D-DOX_{ADH}.

cleaved the acid-labile dynamic covalent bonds in the dimers. The carbamate conjugation in the D-DOX_{car} is more stable than the hydrazone bond in the D-DOX_{ADH}; therefore, the D-DOX_{ADH} was easily cleaved in a restricted mode owing to the noncovalent interaction with the D-DOX_{car}. Thus, the remaining D-DOX_{car} dimers were adsorbed on the nanoparticles with the emulsifying effect of the DOX-PEG. As the release time was prolonged, more D-DOX_{ADH} dimers in the hydrophobic cores were cleaved off, a shell layer of the slow-releasing dimer D-DOX_{car} was formed; as a result, a more obvious impeding effect was produced. The drug releasing rate became slower and slower with the increase in time (Fig. 3B).

The drug release data were then fitted with Higuchi and Korsmeyer-Peppas equations to further understand the drug releasing mechanism (Fig. S4). As shown in Table 2, the correlation coefficients from the Higuchi equation were higher than those from the Korsmeyer-Peppas equation in most cases, indicating a better fit with the Higuchi equation of the diffusion mechanism based on Fick's law for water-soluble drugs [18], namely, the released DOX after the cleavage of the dimers in the present study.

Table 2
Fitted parameters with the Higuchi and Korsmeyer-Peppas models.

DSDSs	Releasing media	Higuchi		Korsmeyer-Peppas	
		R ²	k	R ²	n
D-DOX _{mix} -1	pH 5.0 ABS	0.8468	2.1124	–	–
	pH 7.4 PBS	0.8098	0.3210	0.7399	0.3963
D-DOX _{mix} -2	pH 5.0 ABS	0.6644	0.1205	0.7201	0.6130
	pH 7.4 PBS	0.7647	0.0539	0.6101	0.6693
D-DOX _{mix} -3	pH 5.0 ABS	0.9270	1.7625	–	–
	pH 7.4 PBS	0.9247	0.2386	0.9281	0.4921
D-DOX _{mix} -4	pH 5.0 ABS	0.9551	1.0654	0.9430	0.5676
	pH 7.4 PBS	0.9409	0.1502	0.9312	0.4550
D-DOX _{mix} -5	pH 5.0 ABS	0.9637	0.4129	0.9101	0.7759
	pH 7.4 PBS	0.9654	0.0619	0.9411	0.7826

–: no data. ABS: acetate-buffered solution; PBS: phosphate-buffered saline.

3.3. In vitro cellular toxicity and intracellular distribution

The cellular toxicity of the proposed D-DOX_{mix} NPs on the HepG2 cancer cell line was evaluated in vitro after incubation for 24 h, in comparison with the free DOX at different dosages. Similar to that with the free DOX, the cell viability of HepG2 cells decreased with increased dosage of the three kinds of D-DOX_{mix} NPs with similar DOX content from 2.5 to 20 µg/mL (Fig. 4). However, the cell viabilities after incubation with the D-DOX_{mix} NPs were higher than those with the free DOX at the same dosage. At each dosage, the cell viability decreased from the D-DOX_{mix}-1 NPs to the D-DOX_{mix}-5 NPs.

At a dosage of 20 µg/mL, the cell viability was in the range of 52%–58% for the D-DOX_{mix} NPs, whereas it was only approximately 39% after incubation with free DOX. For the D-DOX_{mix}-1 NPs, which were prepared with a D-DOX_{ADH}:D-DOX_{ADH}-PEG feeding ratio of 10:10 (mg/mg) and showed the fastest drug releasing rate among the three samples, the cumulative drug release was 84.5% in the simulated tumor intracellular microenvironment within 24 h (Fig. 3B). After 24 h of incubation, the actual amount of released DOX was calculated to be 9.6 µg/mL, estimated as the multiplication of the DOX content, dosage, and cumulative drug release in 24 h of the D-DOX_{mix}-1 NPs. The D-DOX_{mix}-5 NPs, prepared with a D-DOX_{car}:D-DOX_{ADH}-PEG feeding ratio of 10:10 (mg/mg), showed the

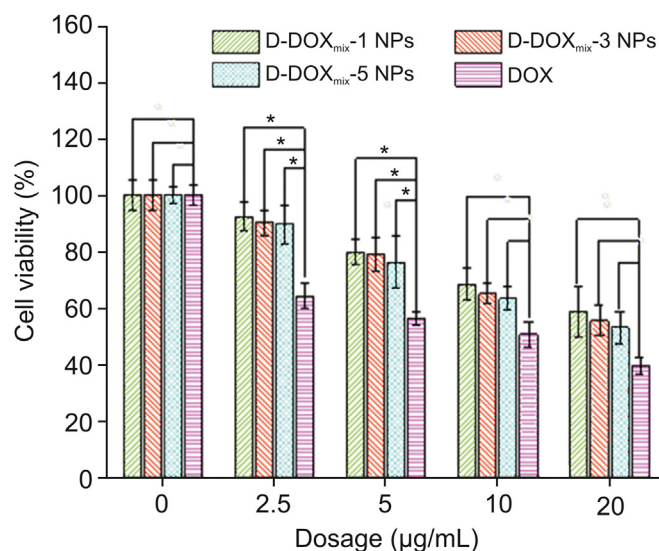


Fig. 4. In vitro cell viability of HepG2 cells against the D-DOX_{mix} NPs and free DOX after incubation for 24 h (*P<0.05).

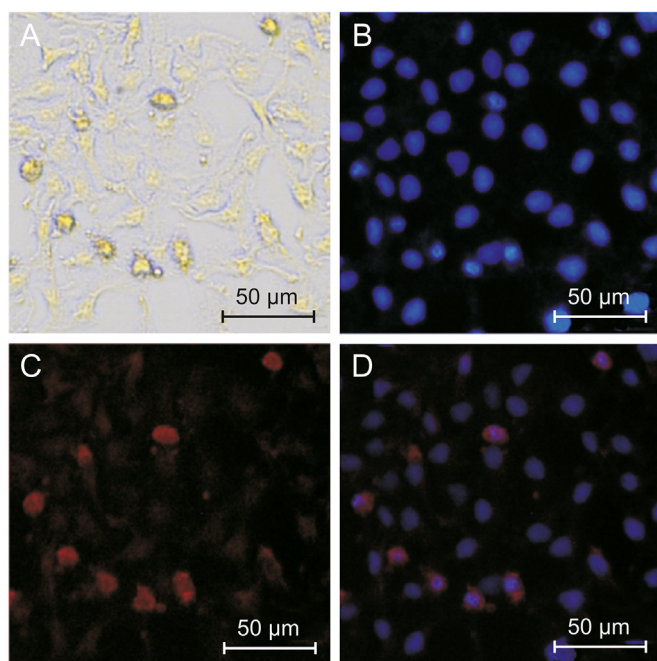


Fig. 5. Confocal laser scanning microscopy images of the HepG2 cells after incubating with the D-DOX_{mix}-3 NPs (15 μg/mL) for 24 h: (A) bright field, (B) 4',6-diamidino-2-phenylindole, (C) DOX, and (D) the merged image.

slowest drug release rate among the three samples, only 4.20% at pH 5.0 within 24 h. The actual amount of released DOX was calculated as 0.5 μg/mL. As for the D-DOX_{mix}-3 NPs prepared with a D-DOX_{car}:D-DOX_{ADH}:D-DOX_{ADH}-PEG feeding ratio of 5:5:10 (mg/mg/mg), a moderate drug release rate was achieved, with a cumulative release of 39.16% at pH 5.0 within 24 h. The actual amount of released DOX was calculated as 4.7 μg/mL. D-DOX_{ADH}-PEG could be cleaved to release DOX and DOX-PEG intracellularly the tumor cells. The D-DOX_{ADH}-PEG content in the D-DOX_{mix} NPs was approximately 50%. The actual amount of released DOX was 1.7 μg/mL in the DOX-PEG if the D-DOX_{ADH}-PEG was completely cleaved off. Considering the complete release of the DOX and DOX-PEG from the D-DOX_{mix} NPs, the actual total amount of released DOX was 11.3, 6.4, and 2.2 μg/mL from the D-DOX_{mix}-1 NPs, D-DOX_{mix}-3 NPs, and D-DOX_{mix}-5 NPs within 24 h, respectively. With the decline in actual total amount of released DOX, increased cytotoxicity was achieved for the three DSDS nanoparticles, demonstrating that the higher cytotoxicity resulted from the slower drug release rate [11]. This was probably caused by the more complete inhibition of the P-gp drug efflux pump with the slow-releasing DSDS nanoparticles. Furthermore, the cell viability of the D-DOX_{mix}-5 NPs was much lower than that of the free DOX at 2.5 μg/mL, indicating an enhanced anti-tumor efficacy of the slow-release mixed DSDS nanoparticles. However, the D-DOX_{mix}-1 NPs showed the lowest actual cytotoxicity, maybe owing to the P-gp drug efflux pump being similar to that of the free drug [19], because of its faster drug releasing rate.

Finally, the *in vitro* cellular uptake and intracellular distribution of the D-DOX_{mix}-3 NPs were assessed using the confocal laser scanning microscopy technique, after incubation of the HepG2 cells with the D-DOX_{mix}-3 NPs (15 μg/mL) for 24 h. Obvious cell shrinkage with less cytoplasm mass could be seen in the bright field image of the HepG2 cells after incubation with the D-DOX_{mix}-3 NPs (Fig. 5A), demonstrating the cytotoxic effect mediated through apoptotic cell death [20]. As seen in Fig. 5B, the blue fluorescence regions are the cell nuclei stained with DAPI, whereas the red fluorescence positions in Fig. 5C show the intracellular distribution

of DOX. In the merged image (Fig. 5D), the red fluorescence positions are completely covered by the blue fluorescence regions, indicating the nuclear accumulation of the released drug in the HepG2 cells [21].

4. Conclusions

In summary, a facile strategy was established to regulate the pH-triggered drug release rate, by fabricating a mixed DSDS with high drug content (>50%) with DOX-DOX dimers (a fast-releasing dimer D-DOX_{ADH} and a slow-releasing dimer D-DOX_{car}), stabilized with D-DOX_{ADH}-PEG. The *in vitro* drug release profiles showed that the drug release rate could be efficiently modulated by adjusting the feeding ratio of the dimers. However, an increased cytotoxicity was achieved for the proposed D-DOX_{mix} NPs with similar DOX content but slower DOX releasing rate in the MTT assays. The results further demonstrated that an enhanced anti-tumor efficacy could be achieved with the slow-release mixed DSDS NPs. Such understanding would provide a new insight into designing a promising nanoformulation with high drug content, excellent acid-triggered drug release, and enhanced antitumor efficacy for future tumor treatment.

CRediT author statement

Jiagen Li: Investigation, Visualization, Data curation; **Xinming Li:** Investigation, Visualization; **Pengwei Xie:** Investigation; **Peng Liu:** Conceptualization, Methodology, Investigation, Writing - Reviewing and Editing, Supervision.

Declaration of competing interest

The authors declare that there are no conflicts of interest.

Appendix A. Supplementary data

Supplementary data to this article can be found online at <https://doi.org/10.1016/j.jppha.2021.03.001>.

References

- [1] M. Gonçalves, S. Mignani, J. Rodrigues, et al., A glance over doxorubicin based-nanotherapeutics: from proof-of-concept studies to solutions in the market, *J. Control Release* 317 (2020) 347–374.
- [2] M. Cagel, E. Grotz, E. Bernabeu, et al., Doxorubicin: nanotechnological overviews from bench to bedside, *Drug Discov. Today* 22 (2017) 270–281.
- [3] H.S. El-Sawy, A.M. Al-Abd, T.A. Ahmed, et al., Stimuli-responsive nano-architecture drug-delivery systems to solid tumor microenvironment: past, present, and future perspectives, *ACS Nano* 12 (2018) 10636–10664.
- [4] C.F. Riber, A.N. Zelikin, Recent advances in macromolecular prodrugs, *Curr. Opin. Colloid Interface Sci.* 31 (2017) 1–9.
- [5] J. Ding, J. Chen, L. Gao, et al., Engineered nanomedicines with enhanced tumor penetration, *Nano Today* 29 (2019), 100800.
- [6] P. Duesberg, R. Stindl, R. Hehlmann, Explaining the high mutation rates of cancer cells to drug and multidrug resistance by chromosome reassortments that are catalyzed by aneuploidy, *Proc. Natl. Acad. Sci. U S A* 97 (2000) 14295–14300.
- [7] Q. Song, X. Wang, Y. Wang, et al., Reduction responsive self-assembled nanoparticles based on disulfide-linked drug-drug conjugate with high drug loading and antitumor efficacy, *Mol. Pharm.* 13 (2016) 190–201.
- [8] J. Khan, A. Alexander, Ajazuddin, et al., Exploring the role of polymeric conjugates toward anti-cancer drug delivery: current trends and future projections, *Int. J. Pharm.* 548 (2018) 500–514.
- [9] P. Xue, J. Wang, X. Han, et al., Hydrophobic drug self-delivery systems as a versatile nanoplatform for cancer therapy: a review, *Colloids Surf. B Biointerfaces* 180 (2019) 202–211.
- [10] L. Gao, G. Liu, J. Ma, et al., Drug nanocrystals: *in vivo* performances, *J. Control Release* 160 (2012) 418–430.
- [11] J. Li, X. Li, P. Liu, Doxorubicin-doxorubicin conjugate prodrug as drug self-delivery system for intracellular pH-triggered slow release, *Colloids Surf. B Biointerfaces* 185 (2020), 110608.
- [12] J. Li, P. Liu, Self-assembly of drug-drug conjugates as drug self-delivery system

- for tumor-specific pH-triggered release, *Part. Part. Syst. Charact.* 36 (2019), 1900113.
- [13] N. Kamaly, B. Yameen, J. Wu, et al., Degradable controlled-release polymers and polymeric nanoparticles: mechanisms of controlling drug release, *Chem. Rev.* 116 (2016) 2602–2663.
- [14] P. Liu, R. Zhang, M. Pei, Design of pH/reduction dual-responsive nanoparticles as drug delivery system for DOX: modulating controlled release behavior with bimodal drug-loading, *Colloids Surf. B Biointerfaces* 160 (2017) 455–461.
- [15] P. Liu, R. Zhang, Polymer microspheres with high drug-loading capacity via dual-modal drug-loading for modulating controlled release property in pH/reduction dual-responsive tumor-specific intracellular triggered doxorubicin release, *Colloids Surf. A Physicochem. Eng. Aspects* 577 (2019) 291–295.
- [16] M. Hussain, J. Xie, Z. Hou, et al., Regulation of drug release by tuning surface textures of biodegradable polymer microparticles, *ACS Appl. Mater. Interfaces* 9 (2017) 14391–14400.
- [17] D. Aydin, M. Arslan, A. Sanyal, et al., Hooked on cryogels: a carbamate linker based depot for slow drug release, *Bioconjug. Chem.* 28 (2017) 1443–1451.
- [18] M.S. Sangoi, V. Todeschini, M. Steppe, Monolithic LC method applied to festerodine fumarate low dose extended-release tablets: dissolution and release kinetics, *J. Pharm. Anal.* 5 (2015) 137–141.
- [19] Y.K. Lee, J. Choi, W.P. Wang, et al., Nullifying tumor efflux by prolonged endolysosome vesicles: development of low dose anticancer-carbon nanotube drug, *ACS Nano* 7 (2013) 8484–8497.
- [20] X. Yi, X. Lian, J. Dong, et al., Co-delivery of pirarubicin and paclitaxel by human serum albumin nanoparticles to enhance antitumor effect and reduce systemic toxicity in breast cancers, *Mol. Pharm.* 12 (2015) 4085–4098.
- [21] M. Pei, G. Li, K. Ma, et al., Polymeric prodrug microspheres with tumor intracellular microenvironment bioreducible degradation, pH-triggered “off-on” fluorescence and drug release for precise imaging-guided diagnosis and chemotherapy, *Colloids Surf. B Biointerfaces* 177 (2019) 313–320.